Fault-Location Accuracy of Natural Frequencies Using Incomplete HVDC Station Models

Shao-Yin He, Andréa Cozza, Yan-Zhao Xie

Fault-Location Accuracy of Natural Frequencies Using Incomplete HVDC Station Models

Shao-Yin He, *Member, IEEE*, Andrea Cozza, *Senior Member, IEEE*, Yan-Zhao Xie, *Senior Member, IEEE*

***Abstract*—This paper investigates how the accuracy of fault location estimated from a transmission line's natural frequencies is affected by imperfect modeling of HVDC power-converter stations. These systems include a large number of devices each with specific frequency-dependent characteristics, as filters, reactors and surge protection systems. While it is well-known that location errors may ensue from inaccurate termination models, it is not clear to what extent location accuracy is affected when neglecting one or more of these devices. Results show significant differences depending on the kind of transmission line and the reactor inductance. Including reactors is found not to completely avoid errors, proving the need to take into account the reactive behavior of the converter, which strongly varies according to the HVDC technology. A notable source of errors is level repulsion between station and line resonances, a phenomenon observed when the converter station presents self resonances, e.g., due to DC filters and stray capacitances in reactors. Significant loss of sensitivity to the fault position is found in these cases, impairing fault-location resolution. The first, or dominant, natural frequency of the line is more strongly affected by all these phenomena, suggesting that the standard choice of using the dominant resonance may not be an optimal strategy. Higher-order resonances are instead found to be more robust against inaccurate converter models, and appear to be more suitable for accurate fault location in case of uncertainties about the converter model.**

***Index Terms*—Fault location, power-converter station, transmission-line termination, natural frequencies, inaccurate models, level repulsion, self-resonating converter**

I. Introduction

ENSURING the accuracy of fault-location techniques is a major concern in the protection of HVDC power transmission systems [1]–[3]. The literature of traveling-wave methods (TWM) has widely investigated location errors due to inaccurate modeling of the transmission-line propagation parameters, in particular caused by dispersion of the speed of propagation in aerial and ground modes [2].

Although propagation speed is a major contributor to the evolution of fault transients, a line's terminations also play a fundamental role in the transient polarity and shape of surge fronts, and therefore in the accuracy of TWM [4], [5]. Their impact is all the more prominent in determining the frequencies of resonance of a line subject to faults, since they directly depend on the phase-angle of the terminations reflection coefficient [6]–[9]. Fault-location based on these resonances is at the heart of natural-frequency methods, which have been shown to be effective in case of frequency-dependent terminations, since they are insensitive to distortions in transients fronts, as opposed to TWM [10]–[12].

The importance of termination models in fault-location techniques is indeed routinely discussed when dealing with high-impedance faults [13], where variable conditions are considered. In fact, power-converter stations are also known to present variable and complex boundary conditions, due to the different power-conversion architectures available and their design, which in turn depends on power transmission requirements [14]. The presence of multiple frequency-dependent devices such as smoothing reactors, DC filters, and surge-protection devices results in complex terminations that require careful modeling [15]–[20]. In practice, both line propagation and converter-station models are inevitably affected by uncertainty.

As opposed to transmission lines, power-converter stations are highly non-linear active systems, for which numerical modeling of fault transients is far from trivial, a topic that is still debated even in low-frequency settings, where average-value models have been developed to better reproduce the dynamical response of converters [21], [22]. The widely applied CIGRE models have been used in fault-location analysis [23] but were in fact designed to benchmark the power dynamics of HVDC systems [24]. The possibility of deriving equivalent models of converter stations by means of direct measurements is clearly not an easier option when it comes to non-linear devices that need to be tested on-line under realistic operating conditions. Moreover, converter stations are susceptible to be operated in multiple configurations, which would then all need to be individually modeled [25], further complicating this issue.

Against this complex backdrop, converter stations have sometimes been suggested to approximate high-impedance terminations [8], [26], on the basis of the large inductances of smoothing reactors found mostly in LCC systems, even though they behave as low-impedance terminations at low frequencies, while stray capacitances would shunt them at high frequency [17], [18]. In other cases, DC filters have been suggested to be the dominant boundary factor [27], [28], again assuming a high-impedance reactor [12], [29], [30]. Stray capacitances and surge protection devices are typically neglected, assuming that they affect the power converter only in the high-frequency range.

This review of the literature suggests that frequency-dependent converter-station models currently used may be

(Corresponding author : S.-Y. He) This work was supported in part by the National Natural Science Foundation of China under Grant 52007139, Key R&D Program of Shaanxi Province (2022KWZ-16).

S.-Y. He, Y.-Z. Xie, are with the State Key Laboratory of Electrical Insulation and Power Equipment, School of Electrical Engineering, Xi'an Jiaotong University, Xi'an 710049, China (email: shaoyin.he@xjtu.edu.cn; yzxie@xjtu.edu.cn).

A. Cozza is with the Group of Electrical Engineering - Paris (GeePs), CNRS, CentraleSupelec, Université Paris-Saclay, Sorbonne Universités, 3 & 11 rue Joliot-Curie, Plateau de Moulon 91192 Gif-sur-Yvette CEDEX, France (email: andrea.cozza@ieee.org).

inaccurate or incomplete. To the best of our knowledge, no analysis has yet attempted to assess how fault location is affected depending on the degree of accuracy of converter-station models. This paper presents a theoretical analysis aiming at gaining a basic understanding in this issue, by comparing the results obtained with several station models. The analysis is limited to monopolar lines and metallic faults, in order to better focus on the role of the converter-station model by considering a simpler common framework. Bipolar lines would require to consider all possible fault configurations, with further complexity introduced by the coexistence of all-line and faulty-section sets of resonances, the former depending on the overall line length, while the latter only depends on the fault distance [31]. Previous works have indeed also resorted to equivalent monopolar descriptions [5], [23], [30], [32], [33].

For each converter-station model, the natural frequencies of a monopolar line presenting a short-circuit fault are compared to those expected with approximate models, in order to compute the associated location errors. The main goal of these tests is to assess if it is imperative to accurately model converter stations in order to precisely locate faults, or if approximate models may actually be sufficient, under certain conditions. In particular we identify how certain devices, such as reactors and surge capacitances, may affect fault-location accuracy only over certain fault distances, while they could otherwise be neglected.

The paper is organized as follows: Sec. II recalls the fundamental ideas behind natural frequencies, before extending them to the more general case of frequency-dependent terminations, in order to understand how they affect fault location accuracy and sensitivity. Sec. III provides a brief overview of equivalent models for converter stations. Secs. IV to VII explore how fault location is affected when inaccurate models are used, in particular when assuming high-impedance terminations or only modeling smoothing reactors, while Sec. VIII looks at the impact of neglecting stray capacitances in smoothing reactors.

On the one hand, these results prove that detailed models are not always needed to ensure a good location accuracy, in particular for coaxial-cable lines. On the other hand, DC filters and parasitic elements are found to have the ability to disrupt location accuracy even at frequencies far from their expected resonances, and therefore their impact should not be regarded as negligible. Finally, the standard use of the first, or dominant, natural frequency is shown not to be an optimal approach, with higher-order resonances being far less sensitive to inaccurate converter-station models.

II. Natural frequencies

The model used throughout this paper to represent an HVDC monopolar transmission line is shown in Fig. 1. A fault of impedance Z_f is found at a distance L down a transmission line with characteristic impedance Z_c, a propagation speed v and attenuation α. Boundary conditions are set by the reflection coefficient $\Gamma_s = (Z_s - Z_c)/(Z_s + Z_c)$ at its left end, where Z_s is the station input impedance. A low-impedance fault with $Z_f \ll Z_c$ will be assumed, thus setting a reflection coefficient $\Gamma_f \simeq -1$ at the right end of the line.

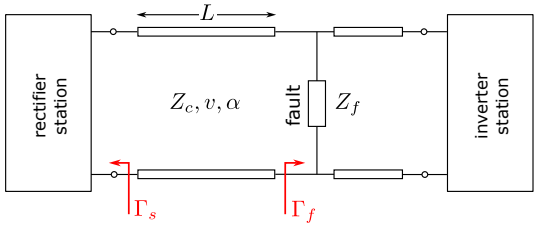

Fig. 1: Monopolar line model used in the analysis of fault-location errors.

A line's resonances, as observed from the rectifier station, are found as solutions to the following equation [6]

$$\Gamma_s \Gamma_f \mathrm{e}^{-\mathrm{j}2sL/v} \mathrm{e}^{-2\alpha L} = 1 \tag{1}$$

where s is Laplace variable and $T = 2L/v$ is the round-trip propagation delay along the line. Solutions can be expressed as $s_n = -1/\tau_n + \mathrm{j}\omega_n$ [34], with ω_n the n-th order natural frequency and τ_n its decay time, caused by losses. Therefore losses have no impact on the natural frequencies, but rather affect the maximum resolution attainable and the resonance excitation [31], [33]. For this reason, propagation losses will be neglected in the rest of the paper, for the sake of simplicity, as they do not provide any insight about the questions set in Sec. I on the effects of inaccurate station models.

The resonance condition (1) is typically recast in terms of the phase-shift angles φ_s, φ_f of the reflection coefficients Γ_s, Γ_f, respectively, [6]

$$\varphi_t = 2\omega_n L/v - \varphi_s(\omega_n) - \varphi_f(\omega_n) = 2k\pi, \tag{2}$$

with $k \in \mathbb{N}$, and typically assuming $k = n$, i.e., a line supports a resonance as soon as the overall (or loop) phase angle φ_t is an integer multiple of 2π.

Solving (2) requires numerical techniques, unless the termination phase-shift angles are independent from the frequency, as often assumed in the literature [6], [35], in which case

$$\omega_n = \frac{2n\pi + \varphi_s + \varphi_f}{2L/v}. \tag{3}$$

A common example is the high-impedance approximation (HZ) for the converter, where $\Gamma_s \simeq 1$ and thus $\varphi_s \simeq 0$ [26], [35], [36]. More realistic termination models result in frequency-dependent values of φ_s.

Given that phase-shift angles are not defined in absolute but rather relative to a reference, (2) is ill-defined. A simple example illustrates this issue: a low-impedance fault could be represented with both $\varphi_f = \pi$ or $\varphi_f = -\pi$, leading to an ambiguity about ω_n as computed from (3), with two different values to choose from. If also the converter termination had a low impedance, this ambiguity would lead to an overall termination phase $\varphi_s + \varphi_f$ equal to -2π, 0 or 2π, resulting in three possible values of ω_n. In short, (2) is correct up to an undefined multiple of 2π.

Therefore, a different approach will be followed in this paper. The resonance ω_n will be found as the n-th solution of

$$\cos\left(2\omega_n L/v - \varphi_s(\omega_n) - \varphi_f(\omega_n)\right) = 1, \tag{4}$$

directly obtained from (1), which no longer requires knowledge of the absolute value of φ_s and φ_f. Numerical techniques are required in solving (4).

A. Location bias

Knowledge of a line's natural frequencies has been extensively used in estimating a fault distance, by inverting (3) [6], [7], [10]–[12]

$$\hat{L}_n = \frac{2n\pi + \hat{\varphi}_s(\omega_n) + \hat{\varphi}_f(\omega_n)}{2\omega_n/v}, \tag{5}$$

from any n-th order resonance. Hatted quantities indicate that termination phase-shift angles are necessarily based on either estimates or assumptions, which might differ from their actual values.

Inevitably, (5) is affected by the same ill-defined use of phase angles discussed for (3). A more robust approach would use (4) to generate a table of the function $f_n : L \mapsto \omega_n$, mapping fault distance into line resonances, which could then be used as a look-up table, translating the resonance ω_n back into the fault distance L. This approach is applied throughout Secs. III to VIII in estimating location errors:

1) a first mapping $f_n : L \mapsto \omega_n$ is established using the actual station termination model;
2) a second mapping $g_n : L \mapsto \omega_n$ is computed using an incomplete station model;
3) the location error is obtained as $\hat{L}_n - L = g_n^{-1}(\omega_n) - L$.

In spite of its shortcomings, (5) still provides one useful insight. Defining $\Delta\varphi = \hat{\varphi}_s + \hat{\varphi}_f - \varphi_s - \varphi_f$ as the overall phase error in the termination models, the location error (or bias) $\Delta L_n = \hat{L}_n - L_n$ is found as

$$\frac{\Delta L_n}{L} = \frac{\Delta\varphi(\omega_n)}{2n\pi + \varphi_s(\omega_n) + \varphi_f(\omega_n)}. \tag{6}$$

This result suggests that the higher the resonance order n, the lower the impact of modeling errors in the line termination phase angles, thanks to an increasing contribution of the propagation to the loop phase angle φ_t, presented by the term $2n\pi$. Secs. V to VII provide clear evidence confirming this prediction and the importance of using higher-order natural frequencies.

B. Sensitivity to fault position

Fault location methods based on natural frequencies rely on the idea that the resonances of a line are sensitive to the fault position [6]. The general case of frequency-dependent terminations may alter this sensitivity, resulting in a risk of loss of spatial resolution [34].

The sensitivity $\mathrm{d}\omega_n/\mathrm{d}L$ can be computed from (2), yielding

$$\frac{\mathrm{d}\omega_n}{\mathrm{d}L} = -\frac{\omega_n}{L}\left[1 - \frac{v(\omega_n)}{2L}\left(\varphi'_s(\omega_n) + \varphi'_f(\omega_n)\right)\right]^{-1} \tag{7}$$

with $\varphi'_s(\omega_n)$ the frequency derivative of $\varphi_s(\omega)$ evaluated at ω_n, whereas $\varphi'_f(\omega_n) \simeq 0$. The term between brackets alters the sensitivity $-\omega_n/L$ commonly expected for a constant-phase termination. The mechanism of sensitivity loss can be understood as follows. For an increasing fault distance, the natural frequency ω_n would decrease, hence for $\varphi'_s < 0$ the termination angle φ_s would increase, thus partially compensating the change in phase from the propagation term in (2). Results in Sec. V confirm this interpretation.

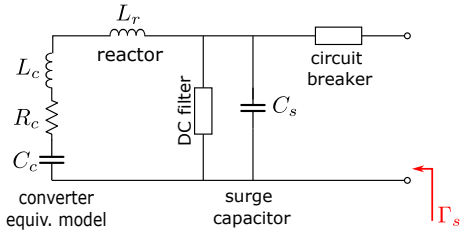

Fig. 2: The complete equivalent model of a HVDC power-converter station connected to a transmission line, used in the analysis of fault-location errors.

III. Converter station models

HVDC power-conversion stations are complex systems that include multiple devices. Across the different conversion technologies currently in use, the model in Fig. 2 provides a framework that takes into account the most common devices: AC/DC converter (rectifier), smoothing reactor, DC filter(s), surge capacitor and circuit breaker. This description is not meant to be exhaustive, but is rather based on the main devices expected to have an impact on fault-location accuracy.

Their characteristics depend on the conversion technology and the power level they are designed for [1], [14]. Line-commutated converter (LCC) stations present the largest smoothing reactors, in the range of 200 to 600 mH, while voltage-source converter (VSC) stations, and in particular modular multi-level converter (MMC) stations, require smaller reactors, typically below 50 mH. The importance of reactors in station models is witnessed by their inclusion in CIGRE models [23], even though those models were designed for benchmarking control strategies, rather than fault-transient propagation [14]. The value of the reactor inductance also plays a major role in identifying whether a fault is internal or external to the converter station [37].

Circuit breakers may also contribute an additional series inductance, meant to limit the current derivative in case of short-circuit faults.

DC harmonics filters are mostly found in LCC and potentially VSC stations [14], [33], but are usually not needed in MMC stations. Their impact on fault transient modeling was discussed in [4], [38], in particular for 12/24-th harmonics filters, as well as in CIGRE models [30]. It is worth noting that DC filters can present very different responses outside their resonant frequencies, with either notch or low-pass filter behavior [14], which would differently affect the station impedance. DC filters are typically associated to overhead transmission lines.

Protection from lightning strikes may require the use of surge capacitances to shunt high-frequency components to the ground, with typical values ranging from 1 to 20 nF [39], [40].

The converter equivalent model covers AC-side components, in particular transformers and filters, and the switching

					coaxial								overhead							
#	converter (Ω,mH,μF)	reactor (mH)	surge cap. (nF)	DC filter	$L_1^{1\%}$ (km)	$L_2^{1\%}$ (km)	$L_1^{10\%}$ (km)	$L_2^{10\%}$ (km)	ϵ_1 %	ϵ_2 %	R_1 %	R_2 %	$L_1^{1\%}$ (km)	$L_2^{1\%}$ (km)	$L_1^{10\%}$ (km)	$L_2^{10\%}$ (km)	ϵ_1 %	ϵ_2 %	R_1 %	R_2 %
1	3/-/-	300	-	-	>55	>490	>665	-	14	2	88	98	>5.5	>51	>69	>676	40	13	82	92
2	3/-/-	30	-	-	>5.5	>50	>67	>656	40	13	82	92	>0.6	>5.1	>6.9	>68	49	13	82	92
3	3/20/-	300	-	-	>51	>528	>701	-	13	1.8	82	92	>7	>55	>73	>720	39	12	82	92
4	3/20/-	30	-	-	>9	>82	>111	-	35	9	82	93	>0.9	>8.5	>11.5	>113	48	12	82	92
5	3/20/80	300	-	-	>58	>520	>605	-	17	1.9	76	97	>6.1	>54	>73	>713	40	12	81	91
6	3/20/80	30	-	-	>9	>82	>108	>864	47	12	60	87	>1	>8.5	>11.5	>113	49	22	82	92
7	3/-/500	300	-	-	>55	>494	>646	-	14	1.9	86	98	>5.7	>51	>69	>675	40	13	82	91
8	3/-/500	30	-	-	>5.5	>49	>66	>636	43	13	80	91	>0.6	>5.1	>6.9	>68	49	23	82	92
9	3/-/-	300	2	-	<0.9	<0.9	-	-	9	8	92	93	<9	<17	< 2.3	< 2.2	160	44	56	89
					>56	>500	>665	-	14	2	88	98	>15	>69	>71	> 678	40	13	82	92
10	3/-/-	300	10	-	<4.1	<4.4	<0.4	<0.4	42	28	73	89	<22	<55	<10	<10	450	40	51	89
					>59	>500	>666	-	14	2	89	98	>29	>108	>79	>686	40	13	82	91
11	3/-/-	300	-	12/24th									>1.3	>11.5	>15	>119	80	55	39	55
12	3/-/-	300	-	6/30th									>0.3	>3.5	>2.6	>34	65	35	39	73

TABLE I: Converter-station configurations tested according to description in Fig. 2 (first vertical tier on the left) and corresponding location-accuracy metrics obtained by assuming a HZ converter-station for a coaxial and a overhead line (second and third tiers). $L_n^{x\%}$ represents the distance range where the n-th line resonance results in a location error exceeding $x\%$. For each range with errors exceeding 1%, ϵ_n is the maximum relative location error observed for the n-th line resonance; R_n the lowest relative sensitivity to the fault position.

network responsible for the DC conversion, including energy storing components such as capacitors. Equivalent models thus differ depending on the conversion technology [1], [24], [41]: purely resistive models may be sufficient for power loss computation [42], but VSC converters include a large DC capacitance C_{DC} from tenths to a few unit mF to reduce harmonic distortion, and its should therefore be included in converter models through an equivalent capacitance. MMC converters use capacitors distributed throughout their N modules, resulting in a lower equivalent capacitance equal to $6C_{DC}/N$. Inductive behavior is also expected because of arm inductances [38]. All these features can be taken into account thanks to average-value models [21], [22], which use a series RLC circuit to represent converters [2], [41], [43], as in Fig. 2.

To the best of our knowledge, the majority of fault-location analysis investigations have not thoroughly explored the potential impact of neglecting converter models, instead mostly focusing on smoothing reactors and DC filters. Secs. IV to VI explore this point, proving that converter models play a non-negligible role in fault-location accuracy. It is also worth noting that converter stations can be operated in multiple ways [25], which would require to consider multiple equivalent models, thus further complicating any analysis.

In the following analysis the state of a converter will be assumed to remain unchanged during the first few ms right after the occurrence of the fault, during which the fault transient is typically measured before being used for estimating the fault location.

IV. Tested station configurations

The brief overview in the previous section highlights that even though converter-station models share similar structures, their equivalent circuits may bear significant differences. As discussed in Sec. II, these differences can be expected to result into potential estimation errors of the termination phase-shift angle φ_s of the converter station and, ultimately, of the line's natural frequencies.

The next sections explore to what extent modeling approximations impact fault location. Sec. V first evaluates location errors caused by approximating a station as a high-impedance (HZ) termination. Sec. VI discusses the case where models only take into account the reactor inductance, while neglecting potential differences in the converter behavior or other devices, based on the assumption that they have a minor impact. Sec. VII instead assumes a HZ reactor, where DC filters would then dominate the station input impedance. Finally, Sec. VIII evaluates the impact of stray capacitances.

Throughout all these sections, a line's natural frequencies are computed for both the exact and approximate converter-station models. As discussed in Sec. II-A, for each natural frequency from the first set (exact model) a fault distance is estimated by using the second set (approximate model) as a look-up table, in order to compute the fault-location accuracy. Across the different scenarios tested, a secondary goal is to conclude if location errors may be negligible for faults within certain distance ranges. In other words, accurate converter-station models may be necessary only for faults beyond or within a threshold distance.

Table I shows the list of configurations tested, with reference to the general model described in Fig. 2. Reactors are the main passive devices typically included in station models. Given the wide range of design choices involved in HVDC systems (cf. Sec. III), two values of reactor inductance are considered, namely 30 and 300 mH, for each configuration tested. The goal is to assess whether detailed converter models can be approximated by simpler models, depending on the value of the reactor inductance.

A series RLC equivalent circuit is used for representing

the converter, as discussed in Sec. III. To the best of our knowledge, fault-location analysis seldom include converter models. A few references have made use of average-value models [2], [41], [43], with one suggesting to use a resistive equivalent model for MMC inverters [42]. In general, it is not clear how fault-location accuracy would be affected by not including converter models.

The configurations tested in the next sections are listed in the first vertical tier of Table I, moving from an ideally purely resistive 3 Ω converter model (#1 and #2) to a partially inductive behavior accounting for the arm inductance from AC transformers (# 3 and #4), while a capacitive behavior needs to be included for MMC (#5 and #6) and VSC converters (#7 and #8). Subsequent configurations extend #1 by including the presence of a surge capacitor (#9 and #10) and of a 12/24-th and 6/30-th harmonics DC filter (#11 and #12).

The internal resistance is assumed to stay low independently from the frequency, even though Caldecott's data point to a growing resistance in VSC tyristors at high frequency, reaching about 400 Ω at 5 kHz [15]. In fact, at that frequency the reflection coefficient phase-shift angle would be dominated by the reactor, even for a 30 mH inductance: a high resistance would thus have a minor impact, making it superfluous to test other values of the converter resistance. Yet, it is unclear if it is entirely correct to assume a low converter resistance below 5 kHz, as experimental results are unfortunately lacking.

For each configuration, two different kinds of transmission line are considered: a) a coaxial cable line (CCL) with a characteristic impedance $Z_c = 25\ \Omega$ and propagation speed $v = 1.8 \times 10^8$ m/s [44], modeling the propagation of phase signals; b) an equivalent monopolar line, modeling the propagation of the aerial (differential) mode of a bipolar overhead line (OHL), with $Z_c = 400\ \Omega$ and $v = 2.9 \times 10^8$ m/s. This choice agrees with the results of the analysis reported in [45], where phase signals where shown to provide the best location accuracy in CCL, while modal signals were found better suited to OHL.

Testing both cases is important, since the same line termination impedance results in significantly different reflection coefficients and therefore affect line resonances differently. Both lines are assumed to be lossless and non-dispersive, for the reasons explained in Sec. II. The main focus will be on the role of the phase angle φ_s of the converter-station models. Fault distances are explored between 0.1 and 1000 km, although distances exceeding 300 km are typically found only in OHL [14], [39], [40]. As discussed in Sec. II, a solid short-circuit fault is assumed.

V. High-impedance approximation

Fig. 3(a) shows the modulus of the input impedance of some of the station models described in Table I. Configuration #1 being based on an ideal 300 mH reactor, it presents a steadily increasing impedance, reaching the characteristic impedance of the OHL ($Z_c = 400\ \Omega$) at 200 Hz, and 13 Hz for a CCL ($Z_c = 25\ \Omega$). In order to approximate a HZ termination, the phase-shift angle φ_s of the station reflection coefficient should ideally be $\varphi_s = 0$. This condition is approximated to within

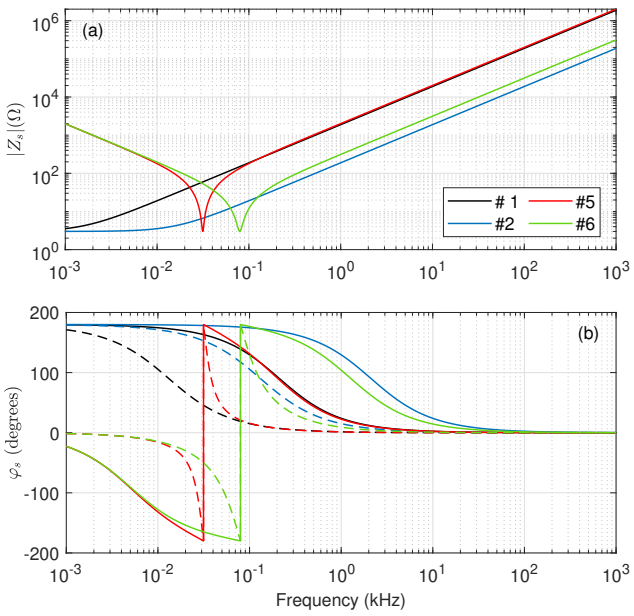

Fig. 3: Comparison of converter station models: (a) modulus of the input impedance for four different models (cf. Table I); (b) phase-shift angle φ_s of the reflection coefficient, assuming an OHL (solid lines) or a CCL (dashed lines).

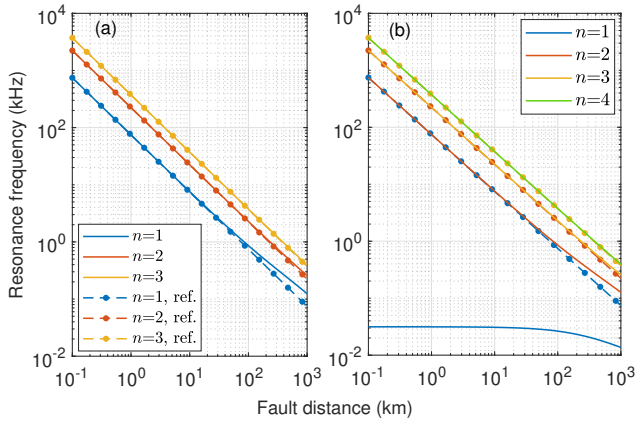

Fig. 4: Natural frequencies for the OHL model for configurations #1 (a) and #5 (b). Dashed lines with circle markers represent the natural frequencies expected for a converter station with HZ, serving as reference in both graphs.

10 degrees above 2.4 kHz and 150 Hz, respectively for an OHL and CCL.

At lower frequencies Fig. 3(b) shows a transition towards $\varphi_s \simeq \pi$, corresponding to a low-impedance termination. This kind of transition has a bearing on fault location, since it was proven in Sec. II-B that the sensitivity of natural frequencies to a fault position decreases in case $\mathrm{d}\varphi_s/\mathrm{d}\omega < 0$. Similar observations apply to #2, involving an ideal 30 mH reactor, but in this case the transition occurs at frequencies about ten times higher.

The first three natural frequencies of the OHL terminated by model #1 are shown in Fig. 4(a) as a function of the fault distance, together with the results expected for a HZ

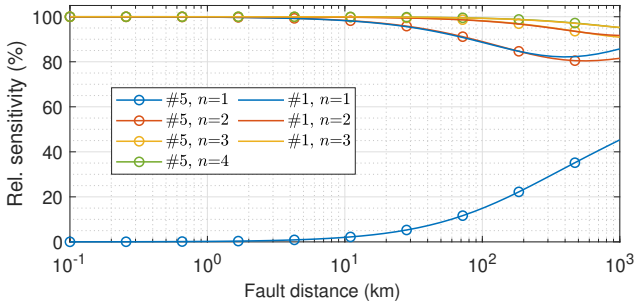

Fig. 5: Sensitivity of the natural frequencies in Fig. 4 to the fault distance. The sensitivity is defined relative to the one expected for the reference model, in this case assuming a high-impedance termination at the converter station.

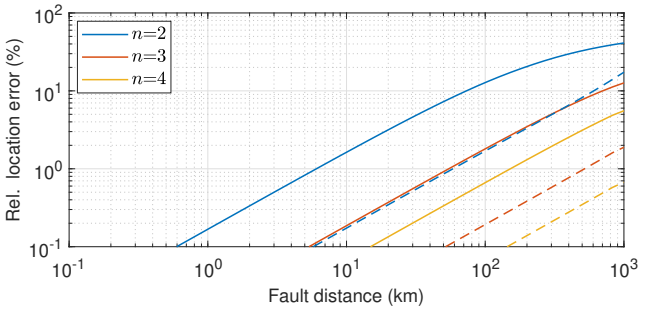

Fig. 6: Location error for station model #5, when assuming as a reference model a high-impedance termination for the converter station. Results are shown for an OHL (solid lines) and a CCL (dashed lines). The dominant frequency (first-order resonance) was discarded, since it is inconsistent with the natural frequencies of the reference model.

termination. As expected the two sets of results closely agree at high frequency, where the station model presents a high input impedance. In spite of this apparently close agreement, Table I indicates that location errors exceed 1% for faults at least 55 km distant for a CCL, and 5.5 km for an OHL. The error reaches 10% at 665 and 69 km, respectively.

Higher-order line resonances better agree with the reference HZ model, with the second resonance displaying a 1% error only beyond 490 km for a CCL and 51 km for an OHL, i.e., about ten times further than the first resonance. This improvement is not due to the second-order resonance occurring at higher frequency, where the reactor impedance would be higher, as argued in Sec. II-A. Indeed, sampling the curves in Fig. 4(a) at a fixed frequency, e.g., at 200 Hz, the second resonance shows a better agreement between the exact and reference models. This observation has practical importance, since it implies that when using higher-order resonances the validity of the HZ termination approximation would hold over larger fault distances

When the reactor has a 30 mH impedance, as in #2, Table I shows that the distances over which 1% and 10% errors are observed are cut down by a factor ten, for both CCL and OHL, thus strongly reducing the viability of the HZ approximation only to close-range faults, within less than 10 km.

The sensitivity of a line's resonances to the fault position, relative to that expected for a constant φ_s (cf. Sec. II-B), is shown in Fig. 5. For #1 there is no major loss of sensitivity, at worst decreasing at 82% for faults at least 200 km distant along an OHL. Similar results are reported in Table I for the 30 mH reactor considered in #2.

Models #3 and #4 include a 20 mH series inductance to the converter model, representing the arm inductance from the AC transformers. Table I reports very similar errors comparing #1 and #3, while a measurable improvement is observed for #4 compared to #2, where the 20 mH inductance significantly increases the input impedance of the station, thus making the HZ approximation more accurate.

A more notable change is observed for models #5 and #6, which include a 80 μF series capacitance, modeling the equivalent capacitance of MMC converters. Their high-frequency behavior is still similar to cases #1 and #2, approximating a HZ termination, but presents a low-frequency capacitive behavior, with a low-impedance resonance at 30 and 80 Hz, respectively, as visible in Fig. 3(a). This resonance leads to a steeper variation of φ_s in Fig. 3(b), and therefore a very significant loss of sensitivity to the fault position, as confirmed by the results in Fig. 4(b) for the first natural frequency[1]. Hence, the first line resonance would be ineffective for locating faults in this case, as it hardly changes with the fault distance. More important is the fact that this first resonance cannot be predicted within the frame of the HZ approximation. Fig. 4(b) shows that subsequent resonances closely agree with those expected for a HZ converter. In the following, we will neglect the first resonance of models #5-#8, all sharing this behavior.

Following this choice, location errors for model #5 are shown in Fig. 6 to exceed 1% for faults further than 6 km and 58 km from the station, for an OHL and a CCL, respectively, using the second resonance. When using the third one, the location accuracy greatly improves, with errors smaller than 1% for faults up to 54 km and 520 km, for an OHL and a CCL, respectively, while still assuming a HZ termination in the reference model. Therefore, discarding natural frequencies due to self-resonant converters leads to a performance similar to the one observed with previous converter models. Fig. 5 confirms that the loss of location sensitivity is also similar. Table I extends these conclusions to model #6.

Similar conclusions are drawn from the analysis of models #7 and #8 which present a converter with a dominant capacitive behavior, with a 500 μF capacitance consistent with VSC converters. Results in Table I again confirm that these models have errors similar to previous cases.

Across the results for all these cases, it appears that the main parameter dictating the location error for a CCL is the reactor inductance. Errors grow much faster in case of a 30 mH reactor (even-numbered models), with the first line resonance attaining a considerable10% error typically within less than a 100 km distance, compared to more than 600 km for a 300 mH reactor (odd-numbered models). These distances are reduced by a factor ten for an OHL, since its higher characteristic impedance strongly limits the validity of the HZ

[1]This phenomenon was explained in Sec. II-B

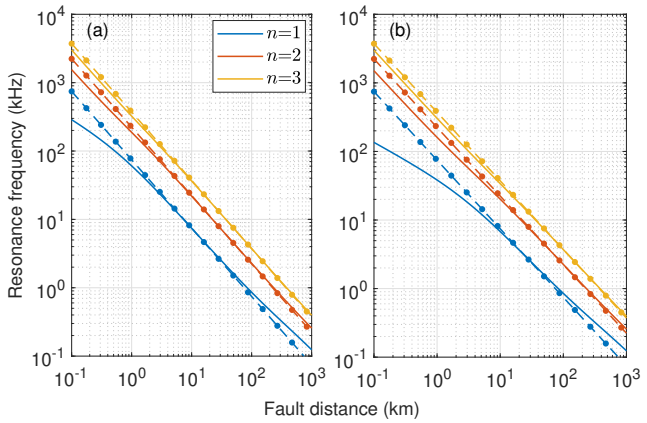

Fig. 7: Natural frequencies for an OHL with station model #9, including a 2 nF (a) and 10 nF (b) surge capacitance.

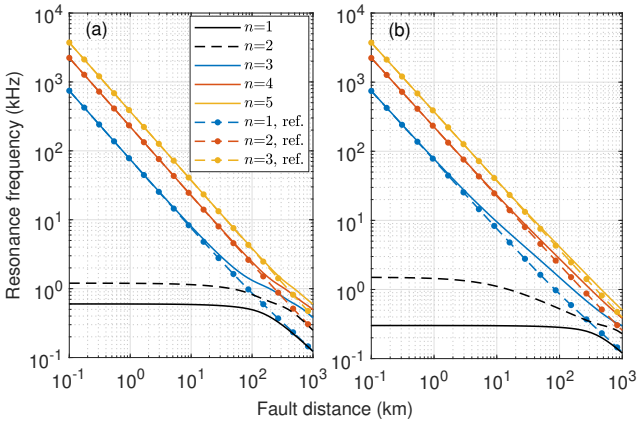

Fig. 8: Natural resonances for the OHL when including a DC filter for: (a) 12/24-th harmonics (#11), (b) 6/30th harmonics (#12). Model #1 serves as reference in both cases.

approximation. The accuracy of the HZ approximation largely improves when switching to the second line resonance, with location errors now reaching 10% at distances ten times larger than with the first resonance for a OHL, and exceeding 600 km for a CCL, even with a 30 mH reactor.

When including surge capacitances, the station input impedance would decrease with the frequency, thus altering the phase angle φ_s. Since at high frequency reactors present a HZ, no significant difference were observed with 30 or 300 mH reactors. Therefore, the effect of surge capacitances can be expected to be decoupled from those examined so far, which were prevalently occurring at the low-frequency end, i.e., for distant faults.

Models #9 and #10 are based on #1, adding respectively a 2 nF and 10 nF surge capacitance. Fig. 7 shows that the line resonances drift away from those for a HZ converter over two separate regions: at large distances as already observed in Fig. 4(a) for #1 (i.e., without the surge capacitance) and at close distances, where the surge capacitance forces a low termination impedance. Table I shows that indeed a surge capacitance has virtually no impact on the location accuracy for distant faults, apart for a 10 nF capacitance with a OHL. In this case, the HZ approximation reaches a 1% error at 29 km instead of 5.5 km for #1, with no surge capacitance. For the second resonance, the 1% distance passes from 51 to 108 km, while the distance for a 10% error is unaffected.

The effect of surge capacitances is observed for close faults, where errors become noticeable within less than 4 km for the CCL, while for the OHL errors are observed up to 22 km.

The last configurations considered are #11 and #12, which add DC filters to model #1, corresponding to an LCC station. Only an OHL is considered for these cases. Model #11 has a 12/24-th harmonics DC filter. Fig. 8(a) shows how it alters the line resonances compared to model #1. Two effects can be noticed: 1) the first two natural frequencies have very low sensitivity to the fault position, and should therefore be discarded for faults less than 100 km away, as already discussed for models #5 and #6; 2) a very strong deviation from the HZ model, even in higher-order resonances, due to level repulsion [2] [46] between the filter-induced resonances and those expected without the filter. Results reported in Table I attest of the deep negative impact of this DC filter, with the 10% error distances cut by a factor five, down to 15 km, maximal errors increased two-fold for the first viable resonance, and five-fold for the second one. Even having discarded the first two natural frequencies, the sensitivity is reduced by more than half for faults at more than 100 km distance. Fig. 8(b) shows results for #12, where a 6/30-th harmonics filter have an even stronger impact, with Table I reporting that 10% errors are now found already at 2.6 km.

These results prove that level repulsion introduced by DC filters results in notable errors even for line resonances occurring at frequencies ten times larger than the DC filter resonances, where they might be expected to have a limited impact.

VI. Reactor-only models

Since the largest source of errors for distant faults is the reactor finite impedance at low frequency, reactors should be included into station models, especially for technologies relying on smaller reactors. While most references in the literature reportedly do so, there is no data available about the improvement in location accuracy with respect to a HZ converter model. Furthermore, it is not clear whether remaining components in the converter model in Fig. 2 could still introduce significant errors, or if modeling the reactor is sufficient to ensure negligible location errors.

These questions are explored in this section by moving from a HZ-based reference model, to one now including the reactor inductance. Table II describes the different scenarios examined: each configuration is associated to a reference model, including either a 300 mH (#1) or a 30 mH reactor (#2).

Converter model #3 differs from #1 by an additional arm inductance. When using the latter as reference model to locate faults, Table II reports a dramatic improvement compared to

[2] i.e., the tendency of resonances to avoid crossing each other's trajectory

		coaxial						overhead					
# act.	# ref.	$L_1^{1\%}$ (km)	$L_2^{1\%}$ (km)	$L_1^{10\%}$ (km)	$L_2^{10\%}$ (km)	ϵ_1 %	ϵ_2 %	$L_1^{1\%}$ (km)	$L_2^{1\%}$ (km)	$L_1^{10\%}$ (km)	$L_2^{10\%}$ (km)	ϵ_1 %	ϵ_2 %
3	1	-	-	-	-	0.9	0.1	>138	-	-	-	1.4	0.6
4	2	>14	>125	>243	-	11.5	4.5	>1.4	>13	25-96	-	12	4.5
5	1	>632	-	-	-	4.7	0.1	152-460	-	-	-	1.2	0.4
6	2	>14	>127	>845	-	14	2.9	1.4-773	>13	25-94	-	12	4.7
7	1	-	-	-	-	0.8	0.01	-	-	-	-	0.2	0.02
8	2	>230	-	-	-	4.6	0.6	-	-	-	-	0.2	0.04
9	1	<0.9	<0.9	-	-	8.5	8.5	<23	<23	<2.4	<2.3	160	44
10	1	<4.4	<4.4	<0.45	<0.42	42	28	<110	<117	<12	<11	450	48
11	1							>1.7	>15	>21	>142	74	51
12	1							>0.3	>3.5	>2.6	>34	65	35

TABLE II: Location error when using reactor-only converter models. The first column is the actual model under consideration, the second being the associated reference model, detailed in Table I. Error metrics in the second and third vertical tiers are described in Table I.

using a HZ model, with errors systematically lower than 1% for a CCL, while peaking at 1.4% for an OHL, when using the first natural frequency. For model #4, the maximum location error is cut down by a factor three compared to a HZ reference model. Yet, location errors still exceed 10% beyond 243 km for a CCL and between 25 and 96 km for an OHL, pointing out the fact that neglecting a 20 mH arm inductance still leads to very large location errors, for a 30 mH reactor inductance. Also in this case, the second resonance performs better, with a 4.5% maximum error.

For model #5 (MMC converter station), the maximum location error is strongly reduced for the OHL, passing from 40% to 1.2% in the worst case, but for a CCL the improvement is more limited, with errors passing from 17% to 4.7%. Non-negligible errors exceeding 1% are observed between 152 and 460 km for an OHL. Larger errors are found with a 30 mH reactor (model #6), with location errors now exceeding 10% between 25 and 94 km of an OHL, similarly to #4, whereas for a CCL this happens only beyond 845 km. Models #7 and #8 (VSC converter), with a predominant capacitive behavior, present a more sustained improvement, with no significant error observed for an OHL, while for a CCL a 1% error is found at 230 km. As stated in Sec. V, the first natural frequency of the capacitive models was discarded, begin weakly sensitive to the fault location.

These results prove that taking into account the reactor when estimating a fault position is not sufficient to ensure negligible errors. Therefore, the nature of the converter, and its equivalent model need to be included in the reference model in order to keep under control location errors, since they affect the degree of accuracy and the distance range where significant errors are observed. Again, these considerations depend on the fault distance, since over certain distance ranges the error may still be acceptable.

Unsurprisingly, short-range location errors induced by a surge capacitance (#9 and #10) are virtually identical to those found in Table I with a HZ reference model, since the reactor model has little impact at high frequency, where the shunting

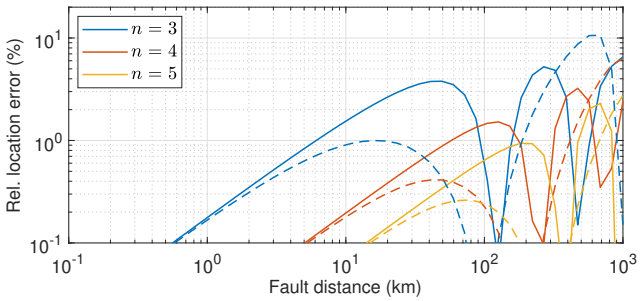

Fig. 9: Location errors when converter stations #11 and #12 are modeled only by their DC filter (with no reactor): 12/24-th (solid lines) and 6/30-th harmonics filter (dashed lines). The first two natural frequencies dominated by the DC filter were not considered, being weakly sensitive to the fault distance.

effect of surge capacitances is expected to affect the station input impedance. Similar observations are found in presence of DC filters (#11 and #12), but for a different reason: the cause is here the strong level repulsion observed in Fig. 8, which cannot be accounted for by simply including the reactor in the reference model.

VII. DC FILTER-ONLY MODELS

The results in Sec. V show that DC filters have a far stronger impact than reactors on fault-location accuracy. A similar conclusion was suggested, without providing evidence, in [33]. Other papers have also suggested that DC filters have a very strong impact on the converter response [20], [47].

We have therefore computed the location accuracy when modeling the converter stations #11 and #12 only by their respective DC filters, assuming a HZ reactor, for an OHL. The first two resonances, induced by the DC filters, were neglected, because of their low sensitivity to the fault position (cf. Fig. 8).

Fig. 9 shows that for #11 (12/24 filter) location errors are lower than 1% only for faults at less than 6 km, and over the ranges 92-158 km and 416-578 km, with errors exceeding 5% above 260 km. For #12 (6/30 filter) location errors do not exceed 1% for faults at less than 178 km and over the range 902-1000 km, with very large errors exceeding 10% over the range 540-697. Higher-order resonances again prove to better accommodate approximate models, with peak location errors cut by half when using the fourth line resonance instead of the third. These results only partially support the idea that LCC stations can be modeled just by their DC-filters, because location errors cannot be regarded as negligible, being in excess of 1%.

VIII. STRAY CAPACITANCES

Further potential sources of location errors can be expected from the non-ideal high-frequency behavior of devices as reactors and circuit breakers. Turn-to-turn stray capacitances are known to exist in reactors, as well as toward surrounding systems, in particular grounded conductors [48]–[51]. Equivalent models introduce a leakage capacitance in parallel to a device,

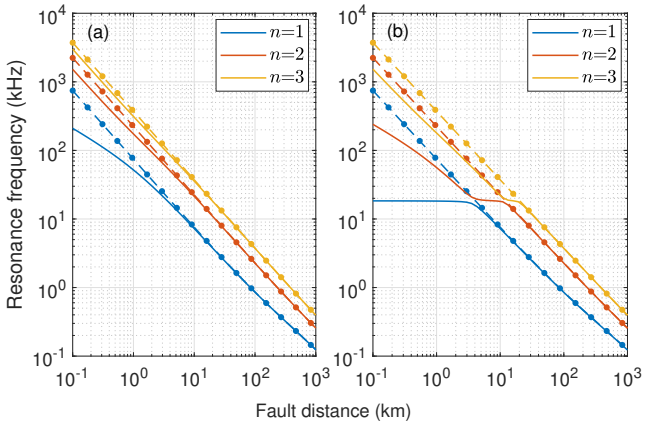

Fig. 10: Natural frequencies of an OHL when taking into account 2 nF leakage and stray capacitances in the reactor, for converter models #1 (a) and #3 (b). Reference results (dashed lines with circles) correspond to results without parasitic elements.

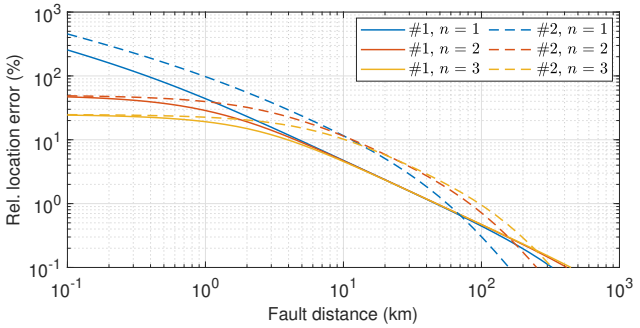

Fig. 11: Location error for 2 nF leakage and shunt capacitances in the reactor of #1 (300 mH) and #2 (30 mH), for a OHL. Errors computed by using reference models including the reactors, but neglecting stray capacitances.

and shunt capacitances connecting each end to the ground. For reactors, the value of leakage and shunt capacitances depend on the geometry, technology and voltage they are designed for. Typical values ranging from 1 nF to 5 nF have been reported for both leakage and shunt capacitances [15], [52], [53]. For isolation switches and circuit breakers smaller stray capacitances around 0.1 nF have been reported [54]. Leakage capacitances need not be taken into account since they are short-circuited, because isolation switches and circuit breakers do not open immediately during a fault transient.

As the frequency increases, stray capacitances would reduce the input impedance of the converter station, similarly to the case of surge capacitors discussed in Sec. V. Since the effect of 2 nF surge capacitances was found to be marginal, it can be expected that no measurable effect will be observed for isolation switches and circuit breakers with 0.1 nF stray capacitances. We will therefore focus on reactors, assuming the same value of 2 nF for both leakage and shunt capacitances, in order to compare this case to that of a 2 nF surge capacitance. The reference converter model is assumed to be perfectly known, but does not include stray capacitances.

Fig. 10(a) compares the natural frequencies of the OHL for converter model #1 with an ideal reactor (reference model), and when affected by stray capacitances. Comparing these results to those for a 2 nF surge capacitance in Fig. 7(a) shows a stronger effect by the reactor's stray capacitances, due to the joint action of leakage and shunt capacitances. Fig. 11 indicates that location errors exceeding 1% are found for faults within 100 km of the converter, corresponding to a broadly constant 1 km location bias. Similar results were obtained with a 30 mH reactor. Location errors were found to be negligible (<1%) for a CCL.

Very different results are found when dealing with an inductive converter model, as in the case of an arm inductance in model #3. The conditions for a self-resonating converter model are now met, creating hybrid resonances with significant level repulsion, as visible in Fig. 10(b). As such, even with a precise converter model including parasitic effects, the first natural frequency would present low location sensitivity for faults within 5 km from the station. Conversely, neglecting parasitic effects would imply attempting to explain the solid-line results in Fig. 10(b) from the point of view of the separate resonances of the reference model, leading to prohibitively large errors. This complex scenario simplifies for faults at least 10 km away from the converter, with natural resonances converging back to the expected low-frequency behavior of an ideal reactor.

IX. Conclusions

This paper has endeavoured to understand how fault-location errors depend on the degree of accuracy in converter station models used in natural frequency-based methods. The first goal was to understand under what circumstances a converter can be approximated by a high-impedance termination. Results have shown that location errors along CCL do not exceed 1% only for fault less than 6 km away for a 30 mH reactor, while for a 300 mH reactor (representative of LCC systems) this range is extended to about 50 km. For OHL these maximum distances are approximatively cut by a factor ten. These results disqualify using the high-impedance approximation for accurate fault location, apart for short-distance transmission lines, such as submarine coaxial cables in off-shore power generation units.

Including reactors in the modeling was then confirmed to substantially improve the accuracy, most notably for the OHL, but still results in very significant errors for a 30 mH reactor, attaining 10% errors for faults between 25 and 96 km. Location errors can be expected to be smaller than 1% only over fault distances within a few km for a 30 mH reactor, while for a 300 mH reactor fault can be accurately located beyond 100 km. Much longer distances where found to be accurately estimated when dealing with a CCL. Outstanding differences were reported among converter models representing different HVDC technologies, depending on the presence of reactive components, such as arm inductances and energy-storage devices found in VSC-based converters.

These conclusions hold practical importance for VSC-based technologies relying on smaller reactors, which cannot be

expected to lead to a high-impedance termination for the converter station. Moreover, station models featuring self resonances were found to lead to strong level repulsion, strongly modifying the natural frequencies predicted with simpler converter models. This phenomenon was found to affect natural frequencies even far from those of the converter self resonances, e.g., those of DC filters. These results alert against the risk of choosing to neglect devices on the basis of a perceived minor impact.

Throughout all these results, higher-order resonances were found to systematically feature better location accuracy and sensitivity, with a higher robustness against the effects of using inaccurate termination models.

Finally, high-frequency phenomena due to stray and surge capacitances were observed only for faults less than 10 km down a transmission line, with a typical absolute location error around 1 km. Similar absolute errors were found when taking into account stray capacitances in reactors, with a measurable impact below 100 km distances.

These results shed some light on the issue of how accurate converter models need to be in order to enable precise fault location. In particular they highlight the impact of neglecting the reactive nature of converters such as in VSC and MMC converters. We expect these conclusions to help engineers in improving line protection techniques to ensure a better performance and ability to accurately locate faults, without necessarily resorting to complex numerical modeling of converter stations. Future work will extend these results to bipolar overhead lines, taking into account additional phenomena enabled by multi-modal propagation, as well as differences between pole-to-pole and pole-to-ground faults.

REFERENCES

[1] M. Muniappan, "A comprehensive review of DC fault protection methods in HVDC transmission systems," *Protection and Control of Modern Power Systems*, vol. 6, no. 1, pp. 1–20, 2021.

[2] W. Xiang, S. Yang, G. P. Adam, H. Zhang, W. Zuo, and J. Wen, "DC fault protection algorithms of MMC HVDC grids: fault analysis, methodologies, experimental validations and future trends," *IEEE Trans. Power Electron.*, 2021.

[3] R. Dashti, M. Daisy, H. Mirshekali, H. R. Shaker, and M. H. Aliabadi, "A survey of fault prediction and location methods in electrical energy distribution networks," *Measurement*, vol. 184, p. 109947, 2021.

[4] N. G. Hingorani, "Transient overvoltage on a bipolar HVDC overhead line caused by DC line faults," *IEEE Trans. Power App. Syst.*, no. 4, pp. 592–610, 1970.

[5] X. Liu, A. Osman, and O. Malik, "Hybrid traveling wave/boundary protection for monopolar HVDC line," *IEEE Trans. Power Del.*, vol. 24, no. 2, pp. 569–578, 2009.

[6] G. Swift, "The spectra of fault-induced transients," *IEEE Trans. Power App. Syst.*, no. 3, pp. 940–947, 1979.

[7] E. Styvaktakis, M. Bollen, and I. Y. Gu, "A fault location technique using high frequency fault clearing transients," *IEEE Power Engineering Review*, vol. 19, no. 5, pp. 58–60, 1999.

[8] G. Bathurst, J. Arrillaga, N. Watson, and A. Wood, "Advanced modelling of the harmonic impedances of AC-DC converters," *IEE Proceedings-Generation, Transmission and Distribution*, vol. 149, no. 6, pp. 700–704, 2002.

[9] M. Farshad, "Locating short-circuit faults in HVDC systems using automatically selected frequency-domain features," *International Transactions on Electrical Energy Systems*, vol. 29, no. 3, p. e2765, 2019.

[10] Z.-Y. He, K. Liao, X.-P. Li, S. Lin, J.-W. Yang, and R.-K. Mai, "Natural frequency-based line fault location in HVDC lines," *IEEE Trans. Power Del.*, vol. 29, no. 2, pp. 851–859, 2013.

[11] G. Song, X. Chu, X. Cai, S. Gao, and M. Ran, "A fault-location method for VSC-HVDC transmission lines based on natural frequency of current," *International Journal of Electrical Power & Energy Systems*, vol. 63, pp. 347–352, 2014.

[12] V. P. Dardengo, P. A. Cavalcante, and M. C. de Almeida, "An evaluation of wave speed impacts on fault location methods for HVDC lines," in *2018 IEEE PES Transmission & Distribution Conference and Exhibition-Latin America (T&D-LA)*. IEEE, 2018, pp. 1–5.

[13] A. Ghaderi, H. L. Ginn III, and H. A. Mohammadpour, "High impedance fault detection: A review," *Electric Power Systems Research*, vol. 143, pp. 376–388, 2017.

[14] D. Jovcic, *High voltage direct current transmission: converters, systems and DC grids*. John Wiley & Sons, 2019.

[15] R. Caldecott, R. V. DeVore, D. Kasten, S. Sebo, and S. Wright, "HDVC converter station tests in the 0.1 to 5 MHz frequency," *IEEE Trans. Power Del.*, vol. 3, no. 3, pp. 971–977, 1988.

[16] F. L. Luo, J. Li, Z. J. Xu, Y. Li, J. Zhang, and S. F. Liu, "Study on impedance-frequency characteristics of HVDC filter commutate converter," in *2008 Third International Conference on Electric Utility Deregulation and Restructuring and Power Technologies*, 2008, pp. 1652–1656.

[17] G. Song, X. Cai, S. Gao, J. Suonan, and G. Li, "Natural frequency based protection and fault location for VSC-HVDC transmission lines," in *2011 International Conference on Advanced Power System Automation and Protection*, vol. 1. IEEE, 2011, pp. 177–182.

[18] G. Song, X. Chu, X. Cai, and S. Gao, "A novel pilot protection principle for VSC-HVDC cable lines based on fault component current," *International Journal of Electrical Power & Energy Systems*, vol. 53, pp. 426–433, 2013.

[19] C. Zhang, G. Song, T. Wang, and L. Yang, "Single-ended traveling wave fault location method in DC transmission line based on wave front information," *IEEE Trans. Power Del.*, vol. 34, no. 5, pp. 2028–2038, 2019.

[20] B. Li, J. He, Y. Li, and B. Li, "A review of the protection for the multi-terminal VSC-HVDC grid," *Protection and Control of Modern Power Systems*, vol. 4, no. 1, pp. 1–11, 2019.

[21] H. Saad, J. Peralta, S. Dennetiere, J. Mahseredjian, J. Jatskevich, J. Martinez, A. Davoudi, M. Saeedifard, V. Sood, X. Wang *et al.*, "Dynamic averaged and simplified models for MMC-based HVDC transmission systems," *IEEE Trans. Power Del.*, vol. 28, no. 3, pp. 1723–1730, 2013.

[22] N. Chen, L. Qi, W. Hou, and X. Cui, "Average value model of modular multilevel converters for switching overvoltage simulation in VSC-HVDC grids," *IEEJ Transactions on Electrical and Electronic Engineering*, vol. 14, no. 8, pp. 1153–1163, 2019.

[23] F. Dehghan Marvasti, A. Mirzaei, and M. E. Hamedani Golshan, "Novel pilot protection scheme for line-commutated converter high voltage direct current transmission lines based on behaviour of characteristic harmonic impedances," *IET Generation, Transmission & Distribution*, vol. 15, no. 2, pp. 264–278, 2021.

[24] P. Sun, F. Arrano-Vargas, H. R. Wickramasinghe, and G. Konstantinou, "Benchmark models for HVDC systems and DC-grid studies," in *2019 9th International Conference on Power and Energy Systems (ICPES)*. IEEE, 2019, pp. 1–6.

[25] J. Wu, H. Li, G. Wang, and Y. Liang, "An improved traveling-wave protection scheme for LCC-HVDC transmission lines," *IEEE Trans. Power Del.*, vol. 32, no. 1, pp. 106–116, 2016.

[26] A. Wood and J. Arrillaga, "The frequency dependent impedance of an HVDC converter," *IEEE Trans. Power Del.*, vol. 10, no. 3, pp. 1635–1641, 1995.

[27] X. Zhang, N. Tai, Y. Wang, and J. Liu, "Emtr-based fault location for DC line in VSC-MTDC system using high-frequency currents," *IET Generation, Transmission & Distribution*, vol. 11, no. 10, pp. 2499–2507, 2017.

[28] R. Muzzammel, "Traveling waves-based method for fault estimation in HVDC transmission system," *Energies*, vol. 12, no. 19, p. 3614, 2019.

[29] Y. Zhang, N. Tai, and B. Xu, "Fault analysis and traveling-wave protection scheme for bipolar HVDC lines," *IEEE Trans. Power Del.*, vol. 27, no. 3, pp. 1583–1591, 2012.

[30] S. Luo, X. Dong, S. Shi, and B. Wang, "A directional protection scheme for HVDC transmission lines based on reactive energy," *IEEE Trans. Power Del.*, vol. 31, no. 2, pp. 559–567, 2015.

[31] A. Cozza, S.-Y. He, and Y.-Z. Xie, "Impact of propagation losses on fault location accuracy in full transient-based methods," *IEEE Trans. Power Del.*, vol. 36, no. 1, pp. 383–396, 2021.

[32] R. Benato, M. Forzan, M. Marelli, A. Orini, and E. Zaccone, "Harmonic behaviour of hvdc cables," *Electric power systems research*, vol. 89, pp. 215–222, 2012.

[33] Z.-Y. He and K. Liao, "Natural frequency-based protection scheme for voltage source converter-based high-voltage direct current transmission lines," *IET Generation, Transmission & Distribution*, vol. 9, no. 13, pp. 1519–1525, 2015.

[34] S.-Y. He, A. Cozza, and Y.-Z. Xie, "On the spatial resolution of fault-location techniques based on full-fault transients," *IEEE Trans. Power Del.*, vol. 35, no. 3, pp. 1527–1540, 2020.

[35] A. Borghetti, M. Bosetti, C. A. Nucci, M. Paolone, and A. Abur, "Integrated use of time-frequency wavelet decompositions for fault location in distribution networks: Theory and experimental validation," *IEEE Trans. Power Del.*, vol. 25, no. 4, pp. 3139–3146, Oct 2010.

[36] P. Chen, B. Xu, and J. Li, "A traveling wave based fault locating system for HVDC transmission lines," in *2006 International Conference on Power System Technology*, 2006, pp. 1–4.

[37] S. Yang, W. Xiang, and J. Wen, "An improved DC fault protection scheme independent of boundary components for MMC based HVDC grids," *IEEE Transactions on Power Delivery*, vol. 36, no. 4, pp. 2520–2531, 2020.

[38] Y. Yang, N. Tai, C. Fan, L. Yang, and S. Chen, "Resonance frequency-based protection scheme for ultra-high-voltage direct-current transmission lines," *IET Generation, Transmission & Distribution*, vol. 12, no. 2, pp. 318–327, 2018.

[39] O. M. K. K. Nanayakkara, A. D. Rajapakse, and R. Wachal, "Location of DC line faults in conventional HVDC systems with segments of cables and overhead lines using terminal measurements," *IEEE Trans. Power Del.*, vol. 27, no. 1, pp. 279–288, 2012.

[40] M. Yang, W. Sima, X. Han, R. Wang, C. Jiang, W. Mao, and P. Sun, "Failure analysis and maintenance of a surge capacitor on the neutral bus in a $\pm$500 kV HVDC converter station," *IET Renewable Power Generation*, vol. 10, no. 6, pp. 852–860, 2016.

[41] C. Zhang, G. Song, and X. Dong, "A novel traveling wave protection method for DC transmission lines using current fitting," *IEEE Trans. Power Del.*, vol. 35, no. 6, pp. 2980–2991, 2019.

[42] U. N. Gnanarathna, A. M. Gole, and R. P. Jayasinghe, "Efficient modeling of modular multilevel HVDC converters (mmc) on electromagnetic transient simulation programs," *IEEE Trans. Power Del.*, vol. 26, no. 1, pp. 316–324, 2010.

[43] W. Leterme, J. Beerten, and D. Van Hertem, "Nonunit protection of HVDC grids with inductive DC cable termination," *IEEE Trans. Power Del.*, vol. 31, no. 2, pp. 820–828, 2015.

[44] S. Nordebo, *Electromagnetic dispersion modeling and measurements for HVDC power cables*, 2011.

[45] W. Leterme, S. Pirooz Azad, and D. Van Hertem, "HVDC grid protection algorithm design in phase and modal domains," *IET Renewable Power Generation*, vol. 12, no. 13, pp. 1538–1546, 2018.

[46] L. Novotny, "Strong coupling, energy splitting, and level crossings: A classical perspective," *American Journal of Physics*, vol. 78, no. 11, pp. 1199–1202, 2010.

[47] M. Faruque, Y. Zhang, and V. Dinavahi, "Detailed modeling of CIGRE HVDC benchmark system using PSCAD/EMTDC and PSB/SIMULINK," *IEEE Trans. Power Del.*, vol. 21, no. 1, pp. 378–387, 2005.

[48] E. Larsen, M. Sublich, and S. Kapoor, "Impact of stray capacitance on HVDC harmonics," *IEEE Trans. Power Del.*, vol. 4, no. 1, pp. 637–645, 1989.

[49] R. Caldecott, Y. Liu, S. A. Sebo, D. G. Kasten, and S. E. Wright, "Measurement of the frequency dependent impedance of major station equipment," *IEEE Trans. Power Del.*, vol. 5, no. 1, pp. 474–480, 1990.

[50] P. Liu, R. Che, Y. Xu, and H. Zhang, "Detailed modeling and simulation of $\pm$500 kV HVDC transmission system using PSCAD/EMTDC," in *2015 IEEE PES Asia-Pacific Power and Energy Engineering Conference (APPEEC)*. IEEE, 2015, pp. 1–3.

[51] W. Leterme, D. V. Hertem, C. Niederauer, and A. Gaun, "On modeling of air-core inductors for dc protection studies," in *The 17th International Conference on AC and DC Power Transmission (ACDC 2021)*, vol. 2021, 2021, pp. 193–198.

[52] Z.-Q. Yu, J.-L. He, R. Zeng, H. Rao, X.-L. Li, Q. Wang, B. Zhang, and S.-M. Chen, "Simulation analysis on conducted emd caused by valves in $\pm$800 kV UHVDC converter station," *IEEE Trans. Electromagn. Compat.*, vol. 51, no. 2, pp. 236–244, 2009.

[53] Y. Wang, Z. Yu, X. Zhang, J. Hu, J. He, and S. Chen, "Stray capacitance of HVDC key devices and its impact on harmonic distribution," in *2016 IEEE Electrical Power and Energy Conference (EPEC)*. IEEE, 2016, pp. 1–6.

[54] A. F. I. et al, "Modeling guidelines for fast front transients," *IEEE Trans. Power Del.*, vol. 11, no. 1, pp. 493–506, 1996.